Chemical compositon of piemontites and reaction relations of piemontite and spessartine in piemontite-quartz schists of central Shikoku, Sanbagawa metomorphic belt, Japan

Autor(en): **Izadyar, Javad**

Objekttyp: **Article**

Zeitschrift: **Schweizerische mineralogische und petrographische Mitteilungen = Bulletin suisse de minéralogie et pétrographie**

Band (Jahr): **80 (2000)**

Heft 2

PDF erstellt am: **29.03.2024**

Persistenter Link: https://doi.org/10.5169/seals-60961

Nutzungsbedingungen

Die ETH-Bibliothek ist Anbieterin der digitalisierten Zeitschriften. Sie besitzt keine Urheberrechte an den Inhalten der Zeitschriften. Die Rechte liegen in der Regel bei den Herausgebern.
Die auf der Plattform e-periodica veröffentlichten Dokumente stehen für nicht-kommerzielle Zwecke in Lehre und Forschung sowie für die private Nutzung frei zur Verfügung. Einzelne Dateien oder Ausdrucke aus diesem Angebot können zusammen mit diesen Nutzungsbedingungen und den korrekten Herkunftsbezeichnungen weitergegeben werden.
Das Veröffentlichen von Bildern in Print- und Online-Publikationen ist nur mit vorheriger Genehmigung der Rechteinhaber erlaubt. Die systematische Speicherung von Teilen des elektronischen Angebots auf anderen Servern bedarf ebenfalls des schriftlichen Einverständnisses der Rechteinhaber.

Haftungsausschluss

Alle Angaben erfolgen ohne Gewähr für Vollständigkeit oder Richtigkeit. Es wird keine Haftung übernommen für Schäden durch die Verwendung von Informationen aus diesem Online-Angebot oder durch das Fehlen von Informationen. Dies gilt auch für Inhalte Dritter, die über dieses Angebot zugänglich sind.

Ein Dienst der *ETH-Bibliothek*
ETH Zürich, Rämistrasse 101, 8092 Zürich, Schweiz, www.library.ethz.ch

http://www.e-periodica.ch

SCHWEIZ. MINERAL. PETROGR. MITT. 80, 199–211, 2000

Chemical composition of piemontites and reaction relations of piemontite and spessartine in piemontite-quartz schists of central Shikoku, Sanbagawa metamorphic belt, Japan

by *Javad Izadyar*[1,2]

Abstract

Chemical composition of piemontite and reaction relations between spessartine and piemontite from the Sanbagawa piemontite-quartz schists in central Shikoku have been studied. The Sanbagawa metamorphic belt was formed during a regional Cretaceous intermediate high-pressure type of metamorphism present throughout Southwest Japan. This study clarifies that the Sanbagawa piemontite-quartz schists can be divided into talc-bearing and talc-free types. Piemontite in the talc-bearing type (Asemi-gawa area) exhibits two zones, whereby average chemical compositions of the core and rim based on the piemontite (Pi), pistacite (Ps) and clinozoisite (Czo) end-members are: $X_{Pi} = 0.26$, $X_{Ps} = 0.09$, $X_{Czo} = 0.65$ and $X_{Pi} = 0.21$, $X_{Ps} = 0.19$, $X_{Czo} = 0.60$, respectively. In the Besshi area, average chemical compositions of the core and rim are: $X_{Pi} = 0.17$, $X_{Ps} = 0.13$, $X_{Czo} = 0.70$ and $X_{Pi} = 0.18$, $X_{Ps} = 0.16$, $X_{Czo} = 0.66$, respectively. However, sometimes Fe^{3+} and Mn^{3+} decrease but Al increases from core to rim. Piemontite in the talc-free type exhibits complex zoning patterns. In the Asemi-gawa area, three zones can be seen: a core: ($X_{Pi} = 0.18$, $X_{Ps} = 0.15$, $X_{Czo} = 0.67$), a mantle: ($X_{Pi} = 0.04$, $X_{Ps} = 0.21$, $X_{Czo} = 0.74$), and a rim: ($X_{Pi} = 0.10$, $X_{Ps} = 0.19$, $X_{Czo} = 0.71$). In the Besshi area, two types of zoning can be identified; in one type a decrease of Mn and Fe and an increase of Al, and in another type Mn increases whilst Al and Fe decrease (from core to rim).

The Sanbagawa belt is one of the most extensively studied metamorphic complexes, and thus, gives a good opportunity for finding a relation between chemical variation of piemontite and changing P, T, fO_2 and bulk composition. In general, the piemontite from the Asemi-gawa region contains higher piemontite and lower pistacite and clinozoisite end-members than that from the Besshi area. By considering the difference of metamorphic grade, similarity of bulk composition and constant oxygen fugacity between two areas, piemontite with higher epidote end-member appears to be stable at the higher grade. Based on textural and chemical evidences two steps in the relation between piemontite and spessartine can be distinguished. Spessartine formation is due to the reaction between piemontite and braunite because of the increasing temperature.

Keywords: high-pressure metamorphism, piemontite, spessartine, Japan, Sanbagawa.

Introduction

Piemontite-quartz schists are highly oxidized manganese-rich metamorphic rocks which have been frequently reported in high-pressure metamorphic belts, for example in Europe (REINECKE, 1986), New Zealand (KAWACHI et al., 1983) and Japan (MINAKAWA, 1992). Studying such rocks is important from different points of view. As source of unusual suites of Mn-rich minerals some of which are rare or unique species (e.g. Mn-rich pyroxene, Mn-rich garnet), it provides the best opportunity to obtain valuable information on the crystal chemistry of unusual minerals, and the chemical variations of high-Mn minerals reveal important information on the metamorphic P-T-t history of the host rocks. Piemontite (Pi), pistacite (Ps) and clinozoisite (Czo) are three end-members which can explain the chemical composition of piemontite within its basic formula $Ca_2(Al, Mn^{3+}, Fe^{3+})_3Si_3O_{12}(OH)$. Piemontite is the Mn end-member of the solid solution and is characterized by a unique pleochroism. Some amounts of Mn^{2+}, Sr and Pb can substitute on the

[1] Department of Geology and Mineralogy, Graduate School of Science, Kyoto University, Kyoto, Japan.
[2] Present address: Department of Geology, Faculty of Science, Zanjan University, Zanjan, Iran. <jav7d@mavara.com>

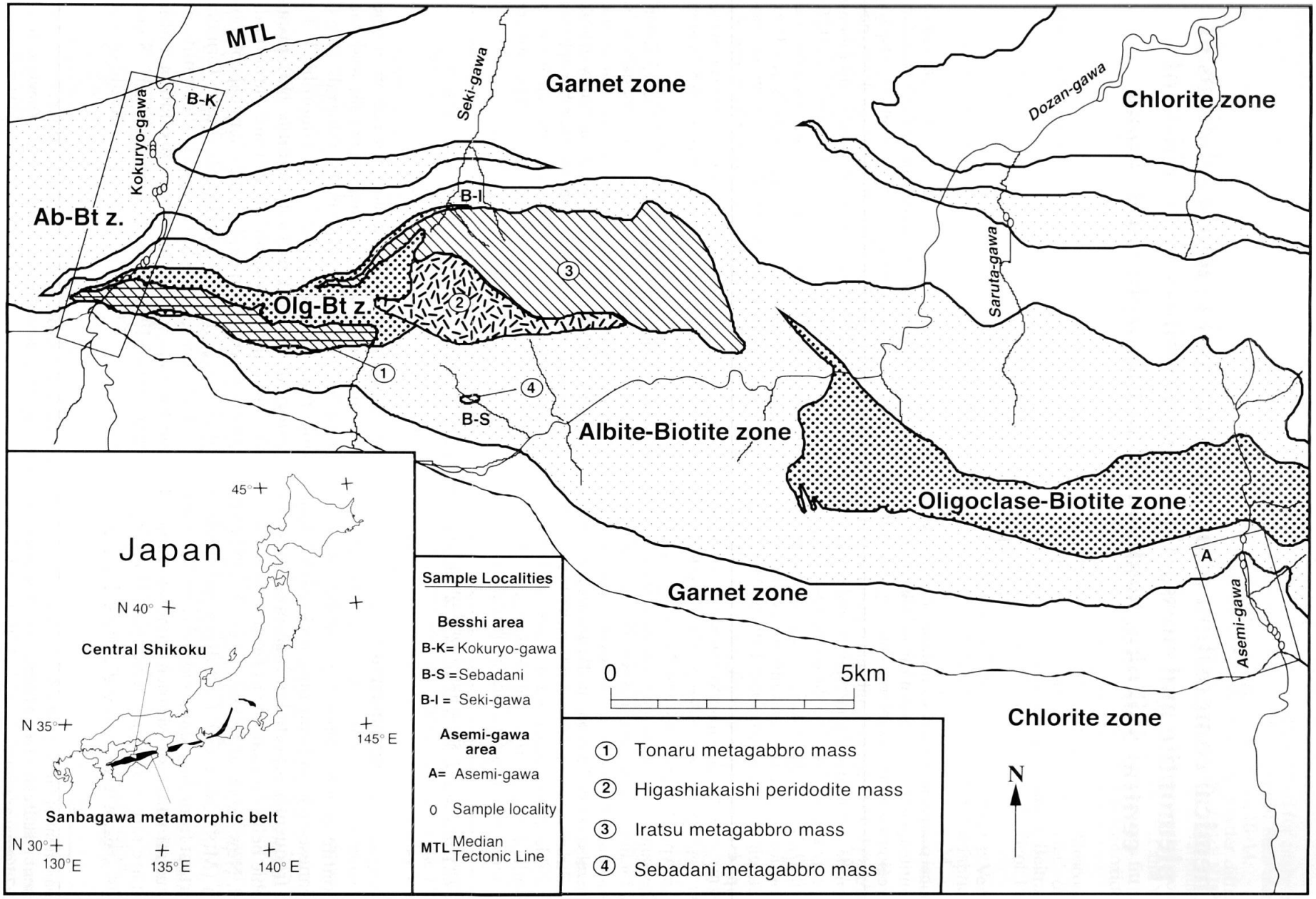


Fig. 1 Geological setting and metamorphic zonal map of the Sanbagawa metamorphic belt in central Shikoku (modified after HIGASHINO, 1990).

Ca site (DEER et al., 1992; KESKINEN and LIOU, 1979; KAWACHI et al., 1983). The chemical composition of natural piemontite varies from 33 mol% $Mn^{3+} + Fe^{3+}$ [Mn^{3+} mol% = $Mn^{3+} \times 100 / (Mn^{3+} + Al + Fe^{3+})$] to 52 mol% which is wider than that of epidote (REINECKE, 1986). The highest Mn^{3+} content has been found for piemontite coexisting with braunite (CHOPIN, 1978) or ardennite (REINECKE, 1986). Experimental investigations on Fe-free piemontite by ANASTASIOU and LANGER (1976, 1977) revealed that piemontite with Al/Mn ratios ranging from 5/1 to 5/7 can be synthesized at the Mn_2O_3–MnO_2 buffer and 7–15 kbar fluid pressure. On the other hand, KESKINEN and LIOU (1979) synthesized piemontite at 2 kbar and fO_2 buffered at Cu_2O/Cu and CuO/Cu_2O, yielding an Al/Mn ratio of 2:1.

In central Shikoku, Sanbagawa belt, Japan, piemontite with variable chemical compositions and complex zoning patterns is abundant in highly oxidized quartz schists. Thus the object of this contribution is to present: chemical composition of piemontites and other Mn-rich minerals from various assemblages; the effect of increasing metamorphic grade on chemical composition of piemontite; the relation between piemontite zonation and Sanbagawa metamorphic conditions; and spessartine-forming reaction derived from textural and chemical evidence.

Geological setting, sample locality and analytical procedure

The Sanbagawa metamorphic belt is an area in Southwest Japan that was subjected to a Cretaceous regional metamorphism of intermediate high pressure (Fig. 1). A large proportion of the Sanbagawa belt consists of metapelites interbedded with varying amounts of oceanic crustal material and is accompanied by ultramafic and mafic tectonic blocks in the highest grade part of central Shikoku (e.g. WALLIS et al., 1992). Quartz schists, e.g., manganiferous and ferrugenous metacherts, are common in the schists (BANNO and SAKAI, 1989). In central Shikoku, the Sanbagawa metamorphic belt is widest and can be divided into four mineral zones; chlorite, garnet, albite-biotite and oligoclase-biotite zones, based on the appearance of index minerals in pelitic schists (e.g. HIGASHINO, 1975; ENAMI, 1983; BANNO and SAKAI, 1989). Metamorphic conditions in this area were estimated at 250–300 °C and 5–6 kbar for the lower chlorite zone, and 610 °C and 10–12 kbar for the oligoclase-biotite zone (BANNO and SAKAI, 1989). Thus, the overall slope of the P-T trajectory from the chlorite zone to the albite-biotite zone is positive (prograde path of metamorphism), but chemical zonation of some minerals such as amphibole and garnet suggest also a retrograde path (BANNO and SAKAI, 1989). For further details on the geology and petrology of this area, the reader is referred to BANNO and SAKAI (1989), HIGASHINO (1990), and WALLIS and BANNO (1990).

The studied samples were obtained from the garnet zone of the Asemi-gawa area and the albite-biotite zone of the Besshi area (Fig. 1).

Chemical analyses were obtained by a scanning electron microscope (Hitachi S550) with a Kevex energy-dispersive X-ray analytical system using the correction subroutine of Magic V program of Kevex 7000 μ system at Kyoto University. Standards were: pure metals for Mn, Cr and Ni; albite, wollastonite and orthoclase for Na, Ca and K; and oxides for Al, Fe, Mg, Ti .

Details of the analytical procedure follow MORI and KANEHIRA (1984) and HIRAJIMA and BANNO (1991). Back-scattered electron (BSE) images were obtained using a GW-BSE detector system of the scanning electron microscope (Hitachi S530 and S550) at 20 kV and a beam current of about 1000 pA.

Petrography

Piemontite-quartz schists from the Asemi-gawa area commonly show compositional banding with alternating piemontite-rich and quartz-rich bands. The width of the piemontite-rich bands ranges from 0.5 to 1.5 mm. They are mainly composed of piemontite, garnet, talc and hematite with subordinate amounts of quartz, phengite, albite and braunite. The quartz-rich bands (1–2 mm thick) mostly contain quartz, phengite, albite, talc and chlorite with minor amounts of piemontite, garnet, hematite and braunite. In comparison to the Asemi-gawa area, samples from the Besshi area do not show clear compositional banding. The Sanbagawa piemontite-quartz schists can be divided into talc-bearing and talc-free types and their mineral assemblages in the relevant areas are as follows (abbreviations following KRETZ, 1983):

Grt zone (Asemi-gawa area): Qtz + Ab + Phn + Chl + Grt + Piemontite + Braunite + Ap + Hem ± Tlc ± Crossite.

Bt zone (Besshi area): Qtz + Ab + Phn + Chl + Grt + Piemontite + Braunite + Ap + Hem ± Tlc ± Barroisite ± Dol.

For comparison, the mineral parageneses of piemontite-quartz schists, pelitic schists and hematite-bearing quartz schists are listed in figure 2.

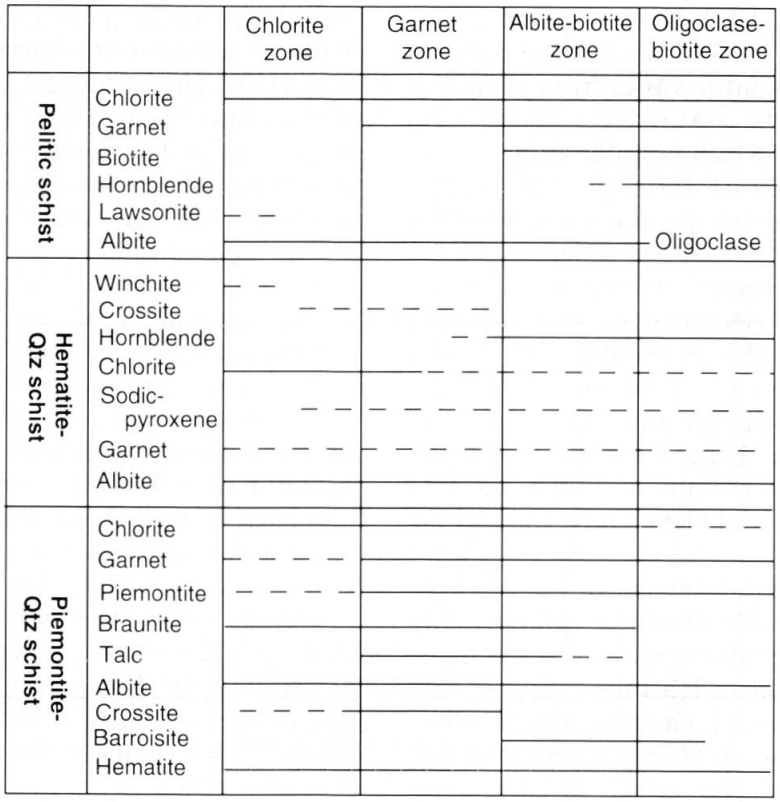


Fig. 2 The stability of silicate minerals in pelitic schists, hematite-quartz schists and piemontite-quartz schists from the Sanbagawa belt. Solid lines: major constituents; dashed lines: minor constituents. Quartz, phengite and epidote are always present. Phlogopite occurs as a secondary mineral in the piemontite-quartz schist. Mineral assemblages of the pelitic schist and the hematite-quartz schist are adapted from ENAMI (1983) and ENAMI et al. (1994).

Tab. 1 Representative analyses of phengite, phlogopite, talc, chlorite and amphibole.

	Asemi-gawa					Besshi			
Point No.	Phengite 18	Chlorite 145	Crossite 739	Phlogopite 1415	Talc 156	Phengite 34	Chlorite 22	Barroisite 17	Talc 44
SiO_2	48.93 (0.04)	30.22 (0.04)	59.17 (0.04)	44.61 (0.04)	63.15 (0.05)	48.18	29.83	54.53 (0.05)	62.73
TiO_2	0.48 (0.01)	–	0.03 (0.00)	–	–	1.07	-	–	–
Al_2O_3	26.28 (0.04)	19.16 (0.03)	7.19 (0.02)	11.15 (0.03)	–	27.71	18.88	6.26 (0.02)	–
Fe_2O_3	3.99 (0.02)	0.78 (0.01)	7.19 (0.03)	0.81 (0.01)	0.07 (0.00)	4.38	0.74	7.39 (0.03)	0.15
Mn_2O_3	0.45 (0.01)	–	0.31 (0.01)	–	–	0.20	–	1.56 (0.01)	–
MnO	–	2.32 (0.02)	–	1.12 (0.01)	0.33 (0.01)	–	1.37 (0.01)	–	0.34
MgO	3.17 (0.02)	31.36 (0.05)	14.69 (0.04)	24.80 (0.04)	30.96 (0.05)	3.17	31.31	17.63 (0.04)	30.93
CaO	–	0.07 (0.00)	0.59 (0.01)	–	–	–	–	5.32 (0.02)	–
Na_2O	0.60 (0.01)	–	7.00 (0.04)	–	–	1.22 (0.02)	–	5.77 (0.04)	–
K_2O	9.53 (0.02)	–	0.05 (0.00)	10.12 (0.03)	–	9.78 (0.03)	–	–	–
Total	93.43	83.91	96.22	92.61	94.51	95.71	82.13	98.46	94.15
	O = 22	O = 28	O = 23	O = 22	O = 22	O = 22	O = 28	O = 23	O = 22
Si	6.67	5.85	8.05	6.36	8.00	6.45	5.90	7.47	8.00
Al^{IV}	1.33	2.15	0.00	1.64	–	1.55	2.10	0.53	–
Al^{VI}	2.89	2.22	1.15	0.23	–	2.82	2.30	0.48	–
Ti	0.05	–	0.003	–	–	0.10	–	–	–
Fe^{3+}	0.40	0.11	0.74	0.09	0.007	0.44	0.10	0.76	0.01
Mn^{3+}	0.05	–	0.03	–	–	0.02	–	0.16	–
Mn^{2+}	–	0.34	–	0.13	0.03	–	0.23	–	0.03
Mg	0.64	9.04	2.98	5.27	5.87	0.63	9.22	3.60	5.89
Ca	–	0.01	0.08	–	–	–	–	0.78	–
Na	0.16	–	1.85	–	–	0.32	–	1.53	–
K	1.66	–	0.01	1.84	–	1.67	–	–	–
Total	13.85	19.72	14.89	15.56	13.90	14.00	19.85	15.31	13.93

Numbers in parentheses indicate precision of each element. Notice that in the Besshi samples only precision is mentioned that differs with the relevant mineral in the Asemi-gawa samples.

Chemical composition of Mn-poor minerals

Talc can be distinguished from phengite by its lower interference colour under the microscope. Talc occurs as a tabular aggregate or as an intercalation with phengite or chlorite. The composition of talc is very close to the ideal formula (Tab. 1).

Phengite, a major phyllosilicate in the studied rocks, occurs both in the matrix and as an inclusion in albite porphyroblasts. Phengite in the Asemi-gawa area is higher in Si than in the Besshi area reflecting the difference of maximum attained temperature during metamorphism (Tab. 1).

Chlorite is in contact with talc and phengite and is commonly associated with piemontite, garnet, braunite and hematite. The composition of the analyzed chlorite is close to the ideal end-member of clinochlore (Tab. 1).

Phlogopite can be found only replacing phengite at the margin in the Asemi-gawa area but is neither in contact with chlorite nor talc. The phlogopite composition deviates from the ideal end-member by excess Si on the tetrahedral site which could be accompanied by excess Al on the octahedral position and a K deficiency (Tab. 1).

The colourless amphiboles in the Asemi-gawa samples occur only as inclusions in albite and garnet porphyroblasts, and their compositions correspond to crossite (Tab. 1). In the Besshi samples they are matrix phases and are magnesiokataphorite or barroisite.

Porphyroblasts of albite commonly contain abundant inclusions of piemontite, hematite, phengite, talc, colourless amphibole, quartz and rarely garnet.

Hematite occurs in the matrix and as inclusions in albite and garnet, and its average composition is $(Fe_{1.90}Mn_{0.08}Ti_{0.01})_{1.99}O_3$. Careful analyses did not reveal any compositional differences between the two areas.

For further details on the chemical composition and the petrographical significance of the talc-phengite-albite assemblage see IZADYAR et al. (2000).

Chemical composition of Mn-rich minerals

PIEMONTITE

Piemontites occur as subhedral and euhedral crystals and show strong pleochroism with X = yellow and Z = pinkish red. Piemontites are present in the matrix as well as enclosed by garnet and albite in piemontite-rich and quartz-rich bands. The structural formula was computed following SMITH and ALBEE (1967) and, for most analyzed piemontites, shows Si = 3.00, Al + Fe^{3+} + Mn^{3+} = 3.00 and Ca = 2.00 per 12.5 oxygens. Therefore, substitution of Al for Si is not indicated by the data. Usually, Mn is present as Mn^{3+} in the octahedral sites but in some piemontites, a certain amount of Mn^{2+} may substitute for Ca.

In piemontites from the talc-bearing schists two zones can be distinguished. The inner zone (core) often forms large crystals; the outer zone is

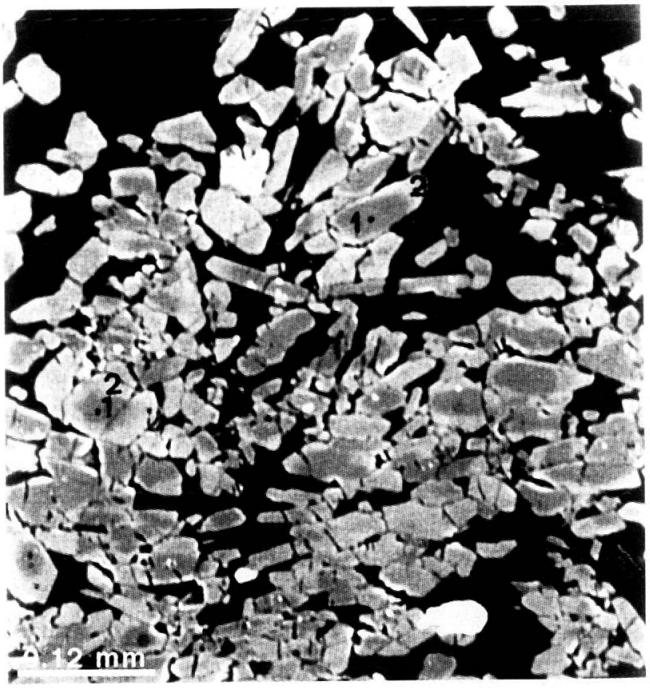


Fig. 3 Back scattered electron image of the piemontite from a talc-bearing piemontite quartz schist. Lighter part (marked by 2) is rim with enrichment of Fe^{3+}-content compared to the darker part (core, labeled by 1).

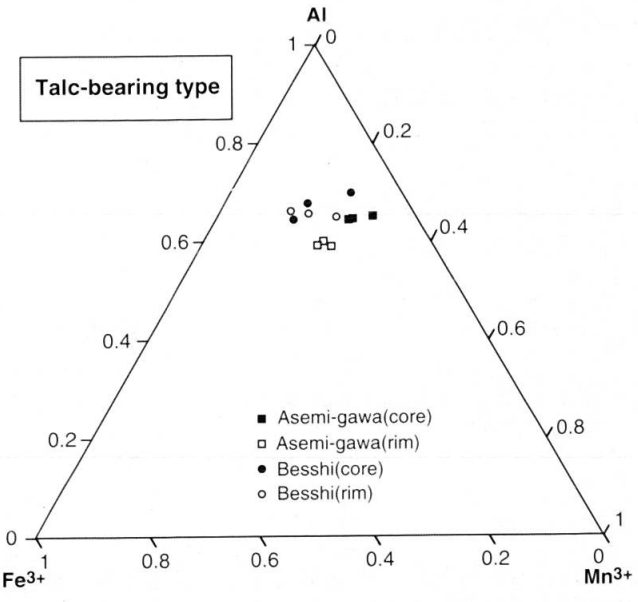


Fig. 4 Chemical composition of the piemontite from the talc-bearing schists.

Tab. 2 Representative analyses of the Asemi-gawa piemontites from the talc-bearing schists.

Point No.	5112	5212	1919	2019	332	132
Core/Rim	Core	Rim	Core	Rim	Core	Rim
SiO_2 wt%	37.74 (0.04)	38.55	38.12	39.00	37.61	38.43
TiO_2	0.11 (0.00)	0.07	0.06	0.07	0.04	0.06
Al_2O_3	20.55 (0.03)	19.07	20.59	19.51	20.30	18.81
Fe_2O_3	2.90 (0.02)	9.78	3.82	9.34	6.11 (0.03)	9.10
Mn_2O_3	14.58 (0.04)	11.75	13.28	12.70	11.35	12.34
CaO	22.99 (0.03)	19.81	22.48	18.98	23.04	19.64
Total	98.87	99.03	98.35	99.60	98.45	98.38
No. of cations based on O = 12.5						
Si	3.01	3.07	3.04	3.08	3.01	3.05
Ti	0.01	0.01	0.01	0.01	0.00	0.01
Al	1.94	1.80	1.94	1.81	1.92	1.78
Fe^{3+}	0.18	0.58	0.24	0.56	0.37	0.55
Mn^{3+}	0.88	0.62	0.81	0.61	0.69	0.67
Total	3.01	3.01	3.00	2.99	2.98	3.01
Ca	1.96	1.69	1.93	1.60	1.98	1.69
Mn^{2+}	–	0.01	–	0.14	–	0.08
Total	1.96	1.70	1.93	1.74	1.98	1.77
End members						
Pi	29.34	20.66	27.00	20.33	23.00	22.33
Ps	6.00	19.33	8.00	18.66	12.33	18.33
Czo	64.66	60.01	65.00	61.01	64.67	59.34

Tab. 2 (cont.) Representative analyses of the Besshi piemontites from the talc-bearing schists.

Point No.	311	312	39	310	45	46
Core/Rim	Core	Rim	Core	Rim	Core	Rim
SiO_2 wt%	37.50 (0.04)	37.82	37.89	37.89	37.58	37.47
TiO_2	–	–	–	–	–	–
Al_2O_3	20.87 (0.03)	21.59	21.25	21.19	21.86	20.15
Fe_2O_3	11.12 (0.04)	10.61	8.89 (0.03)	9.31	4.60 (0.03)	7.17
Mn_2O_3	6.69 (0.03)	6.32	7.03	7.42	10.42	10.93
CaO	20.29 (0.03)	20.63	21.30	20.85	21.98	20.95
Total	96.47	96.97	96.36	96.67	96.44	96.67
No. of cations based on O = 12.5						
Si	2.92	2.92	2.95	2.94	2.90	2.93
Ti	–	–	–	–	–	–
Al	1.92	1.97	1.95	1.94	2.00	1.85
Fe^{3+}	0.65	0.62	0.52	0.54	0.26	0.42
Mn^{3+}	0.40	0.37	0.42	0.44	0.60	0.65
Total	2.97	2.96	2.89	2.92	2.86	2.92
Ca	1.70	1.70	1.77	1.73	1.83	1.75
Mn^{2+}	–	–	–	–	–	–
Total	1.70	1.70	1.77	1.73	1.83	1.75
End members						
Pi	13.33	12.30	14.00	14.66	20.00	21.66
Ps	21.60	20.60	17.33	18.00	8.66	14.00
Czo	65.07	67.10	68.67	67.34	71.34	64.34

Numbers in parentheses indicate precision of each element. Other columns have similar precision as column one, otherwise it is mentioned.
All of the Mn and Fe are considered as Mn_2O_3 and Fe_2O_3.
Mn^{2+} and Mn^{3+} are computed based on structural formula.

a narrow rim surrounding the core (Fig. 3). In the Asemi samples, the rim contains more Fe^{3+} but lower Mn^{3+} and Al than the core (average core composition: $X_{Pi} = 0.26$, $X_{Ps} = 0.09$, $X_{Czo} = 0.65$; average rim composition: $X_{Pi} = 0.21$, $X_{Ps} = 0.19$, $X_{Czo} = 0.60$; $X_{Pi} = Mn^{3+}/(Al + Mn^{3+} + Fe^{3+})$; cf. Fig. 4 and Tab. 2). Inspection of table 2 reveals that the rim is lower in Ca than the core and, in this case, some divalent Mn may substitute for Ca. In the Besshi samples, piemontite does not exhibit clear zoning but sometimes slight zonation could be seen, in which case the rim is richer in Fe^{3+} and Mn^{3+} than the core (average core composition: $X_{Pi} = 0.17$, $X_{Ps} = 0.13$, $X_{Czo} = 0.70$; average rim composition: $X_{Pi} = 0.18$, $X_{Ps} = 0.16$, $X_{Czo} = 0.66$; cf. Fig. 4 and Tab. 2). Sometimes another type of zoning is visible where Fe^{3+} and Mn^{3+} decrease but Al increases from core to rim (cf. points 311–312 in Tab. 2).

Piemontites in the talc-free type show complex chemical zoning patterns. The cores are highly enriched in Mn^{3+} and are surrounded by a mantle which is rich in Al and Fe^{3+}. Zoning is more

Tab. 3 Representative analyses of the Asemi-gawa piemontites from the talc-free schists.

Point No.	136	137	138	131	132	133	11	12	13
Core/Rim	Core	Mantle	Rim	Core	Mantle	Rim	Core	Mantle	Rim
SiO_2 wt%	38.21 (0.04)	37.89	39.96	38.09	38.28	38.65	38.38	38.48	39.24
TiO_2	0.00 (0.00)	0.08	0.00	–	–	0.05	0.04	–	0.03
Al_2O_3	20.04 (0.03)	22.61	22.11	21.32	22.86	22.00	20.97	22.64	22.46
Fe_2O_3	7.59 (0.03)	10.88 (0.04)	8.49	6.52	10.34	9.63	7.52	10.77	10.57
Mn_2O_3	9.44 (0.03)	2.04 (0.02)	5.38 (0.02)	8.90	2.52 (0.02)	4.68 (0.02)	8.58	2.23	3.87 (0.02)
CaO	21.27 (0.03)	23.05	22.25	22.47	23.01	22.83	22.18	23.14	22.89
Total	96.55	96.55	98.19	97.30	97.01	97.84	97.67	97.26	99.06
No. of cations based on O = 12.5									
Si	3.10	3.10	3.10	3.05	3.05	3.05	3.05	3.05	3.05
Ti	0.00	0.01	0.00	–	–	0.01	0.01	–	0.00
Al	1.91	2.14	2.05	2.02	2.15	2.06	1.98	2.14	2.07
Fe^{3+}	0.46	0.66	0.50	0.40	0.62	0.57	0.45	0.64	0.62
Mn^{3+}	0.58	0.12	0.32	0.55	0.15	0.28	0.52	0.13	0.23
Total	2.95	2.93	2.87	2.97	2.92	2.92	2.96	2.91	2.92
Ca	1.85	1.98	1.88	1.94	1.97	1.94	1.90	1.98	1.93
Mn^{2+}	–	–	–	–	–	–	–	–	–
Total	1.85	1.98	1.88	1.94	1.97	1.94	1.90	1.98	1.93
End members									
Pi	19.33	4.00	10.66	18.33	5.00	9.33	17.33	4.33	7.66
Ps	15.33	22.00	16.66	13.33	20.66	19.00	15.00	21.33	20.66
Czo	65.34	74.00	72.68	68.34	74.34	71.67	67.67	74.34	71.68

Tab. 3 (cont.) Representative analyses of the Besshi piemontites from the talc-free schists.

Point No.	16	17	18	19	11	12	28	29
Core/Rim	Core	Rim	Core	Rim	Core	Rim	Core	Rim
SiO_2 wt%	38.35	38.20	37.79	38.33	39.04	40.18	38.58	38.57
TiO_2	–	–	–	–	–	–	–	–
Al_2O_3	22.22	23.02	21.20	22.97	22.23	21.32	22.67	23.30
Fe_2O_3	11.72	12.41	10.77	11.76	12.31	10.63	10.54	12.07
Mn_2O_3	3.24	2.16	5.01	1.32	4.41	6.45	4.07	1.40
CaO	21.89	21.69	21.47	22.19	20.97	20.57	21.85	22.34
Total	97.42	97.48	96.24	96.57	98.96	99.15	97.71	97.68
No. of cations based on O = 12.5								
Si	3.00	2.98	3.00	3.10	2.95	3.00	3.00	3.10
Ti	–	–	–	–	–	–	–	–
Al	2.03	2.17	1.97	2.13	1.98	1.90	2.10	2.10
Fe^{3+}	0.68	0.76	0.70	0.68	0.70	0.60	0.58	0.68
Mn^{3+}	0.19	0.09	0.29	0.08	0.25	0.40	0.30	0.08
Total	2.90	3.02	2.96	2.89	2.93	2.90	2.98	2.86
Ca	1.94	1.89	1.97	1.94	1.70	1.67	1.92	1.94
Mn^{2+}	–	–	–	–	–	–	–	–
Total	7.84	7.89	7.93	7.93	7.58	7.54	7.90	7.90
End members								
Pi	6.33	3.00	9.66	2.66	8.33	13.33	10.00	2.66
Ps	22.66	25.33	23.33	22.66	23.33	20.00	19.33	22.66
Czo	71.01	71.67	67.01	74.68	68.34	66.67	70.67	74.68

Numbers in p arentheses indicate precision of each element. Other columns have similar precision as column one, otherwise it is mentioned. All of the Mn and Fe are considered as Mn_2O_3 and Fe_2O_3. Mn^{2+} and Mn^{3+} are computed based on structural formula.

Tab. 4 Representative analyses of garnet from the talc-bearing schist in the Asemi-gawa area.

	In piemontite-rich band		In quartz-rich band	Enclosed in albite	Changed rim of garnet at contact to matrix			
Point No.	27	43c	130	150	1519	1619	4619	4191
SiO_2 wt%	37.39 (0.04)	37.20	37.46	37.92	37.61	37.33	38.98	39.34
TiO_2	0.23 (0.01)	0.28	0.25	–	0.13 (0.00)	0.14	0.15	0.16
Al_2O_3	19.58 (0.03)	19.01	19.62	19.71	19.21	19.67	19.24 (0.04)	20.67
Fe_2O_3	1.74 (0.02)	1.96	1.73	1.93	4.02 (0.03)	2.65 (0.03)	3.05	3.75
MnO	36.92 (0.06)	36.28	35.71	36.24	25.40 (0.05)	31.03	32.31	28.29
MgO	0.71 (0.01)	0.42	0.57	0.63	0.27	0.17	0.50	0.27
CaO	4.08 (0.02)	3.97	4.47	4.36	12.05 (0.03)	8.95	7.04	9.64
Total	100.65	99.12	99.81	100.79	98.69	99.94	101.27	102.12
No. of cations based on 12 oxygens								
Si	3.04	3.05	3.04	3.04	3.03	3.00	3.07	3.05
Ti	0.01	0.01	0.01	–	0.008	0.003	0.008	0.01
Al	1.86	1.84	1.87	1.87	1.83	1.87	1.89	1.89
Fe^{2+}	–	–	0.07	0.02	0.02	0.11		
Fe^{3+}	0.09	0.12	0.10	0.12	0.17	0.13	0.11	0.11
Mn	2.55	2.52	2.46	2.47	1.74	2.13	2.18	1.86
Mg	0.08	0.05	0.07	0.08	0.03	0.02	0.05	0.03
Ca	0.34	0.34	0.38	0.37	1.04	0.80	0.60	0.80
Total	7.97	7.93	7.93	7.95	7.92	7.97	7.93	7.86
End members								
Sps	85.86	86.60	84.50	84.50	60.40	71.70	76.70	66.42
Pyr	2.70	1.70	2.40	2.74	1.04	0.70	1.60	1.07
Grs	6.84	5.60	8.10	6.76	27.66	20.40	15.50	23.11
And	4.60	6.10	5.00	6.00	8.50	6.50	5.50	5.50
Alm	0.00	0.00	0.00	0.00	2.40	0.70	0.70	3.90

Numbers in parentheses indicate precision of each element. Other columns have similar precision as column one, otherwise it is mentioned.
All of the Fe is considered as Fe_2O_3.
Fe^{2+} and Fe^{3+} are computed based on structural formula.

Tab. 5 Representative analyses of braunite.

Point No.	1832 Asemi-gawa	2032 Besshi-Kokuryo	2132 Besshi-Seki
SiO_2 wt%	10.44 (0.02)	10.34	10.73
TiO_2	0.11 (0.00)	0.15	0.14
Al_2O_3	0.40 (0.02)	0.30	0.35
Fe_2O_3 (total)	12.66 (0.04)	12.35	12.24
Mn_2O_3 (total)	76.38 (0.08)	76.25	77.23
MgO	0.09 (0.00)	0.00	0.08
CaO	0.28 (0.01)	0.26	0.10
Total	100.36	99.65	100.87
No. of cations based on O = 12			
Si	1.02	1.01	1.04
Ti	0.01	0.01	0.01
Al	0.05	0.03	0.03
Fe^{3+}	0.93	0.91	0.89
Mn^{3+}	5.07	5.09	5.37
Mn^{2+}	0.60	0.61	0.53
Mg	0.01	0.00	0.01
Ca	0.03	0.03	0.01
Total	7.72	7.69	7.89

Numbers in parentheses indicate precision of each element. Other columns have similar precision as column one.
Mn^{2+} and Mn^{3+} are computed based on structural formula.



Fig. 5 Back scattered electron image of piemontite from the talc-free piemontite-quartz schist showing three zones: 1 = core with enrichment of Mn^{3+}-content, 2 = mantle with depletion in Mn^{3+}-content, and 3 = rim with enrichment in Mn^{3+}-content.

complicated by the presence of an outer rim which is further enriched in Mn^{3+} (Fig. 5). In the Asemi-gawa area, three generations of piemontites are visible even within one grain. In this case, the core with an average composition of X_{Pi} = 0.18, X_{Ps} = 0.15, X_{Czo} = 0.67 is surrounded by a mantle with an average composition of X_{Pi} = 0.04, X_{Ps} = 0.21, X_{Czo} = 0.74. The mantle, in turn, is surrounded by a rim characterized by X_{Pi} = 0.10, X_{Ps} = 0.19, X_{Czo} =0.71 (cf. Fig. 6 and Tab. 3). In the Besshi piemontites, zonation is not very distinct, but two types may be observed: from core to rim, Mn and Fe decrease and Al increases (cf. points 18–19 and 28–29 in Tab. 3); and Mn increases and Al and Fe decrease (cf. points 11–12 in Tab. 3).

GARNET

Porphyroblasts of garnet occur in both piemontite- and quartz-rich bands. Garnet in piemontite-rich bands is euhedral and its size ranges from 1 to 3 mm. This type of garnet is poikiloblastic, containing many inclusions of piemontite, quartz, hematite, braunite, talc and amphibole. Chemically, these garnets are homogeneous Ca–Fe-bearing spessartines (X_{Sps} = 0.85, X_{Grs} = 0.06 and X_{And} = 0.05). The garnet in quartz-rich bands includes only small amounts of hematite, piemontite and braunite, and garnet is also a Ca–Fe-bearing spessartine (X_{Sps} = 0.84, X_{Grs} = 0.07 and X_{And} = 0.06). In one sample, garnet occurs within an albite porphyroblast in the quartz-rich band and it is chemically the same as that outside albite (Tab. 4).

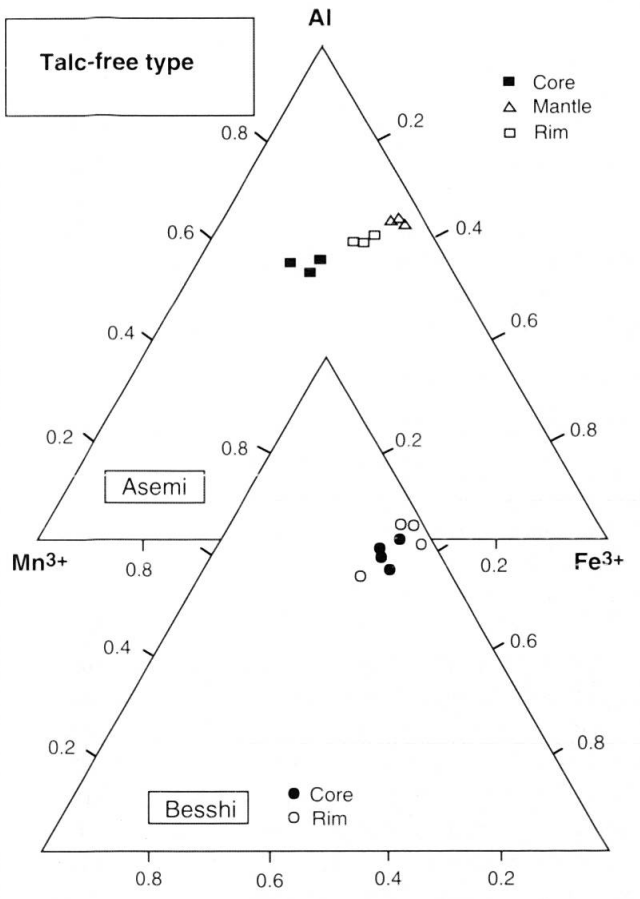


Fig. 6 Chemical composition and compositional variation of piemontite from the talc-free schists.

BRAUNITE

Braunite usually occurs both in the matrix and as inclusions in garnet in the piemontite-rich bands and rarely as inclusions in albite and garnet in the quartz-rich bands. Commonly, it is euhedral and chemically homogeneous. There are no differences between chemical compositions of braunite in the Asemi-gawa and Besshi areas (Tab. 5).

Variation of chemical composition of piemontite with changing metamorphic grade

Experimental investigations on piemontites were performed on Fe^{3+}-free piemontites by ANASTASIOU and LANGER (1976, 1977) and KESKINEN and LIOU (1979), but most of the natural piemontites contain some Fe^{3+}. In order to correlate the experimental results to Fe^{3+}-bearing piemontite, they compared their data to epidote stability studies of HOLDWAY (1972). ANASTASIOU and LANGER concluded that the Mn^{3+}-bearing phase shows higher temperature stability than Fe^{3+}-bearing epidote whilst KESKINEN and LIOU (1979) considered that introduction of Fe in piemontite will extend its stability towards higher temperature. Because the Sanbagawa belt is one of the most extensively studied metamorphic complexes (TAKASU et al., 1994), it provides the best opportunity to study the relation between chemical variation of piemontite and changing P, T, fO_2 and bulk-rock composition. Thus, the samples were collected from the garnet zone in the Asemi-gawa area and albite-biotite zone of the Besshi area. Comparing the average core compositions of piemontites in the talc-bearing type between both areas reveals that the Asemi piemontite is richer in piemontite but poorer in pistacite and clinozoisite components (Asemi-gawa: X_{Pi} = 0.26, X_{Ps} = 0.09, X_{Czo} = 0.65; Besshi: X_{Pi} = 0.15, X_{Ps} = 0.17, X_{Czo} = 0.68; cf. Fig. 4 and Tab. 2). The same results were obtained by comparing average core compositions of piemontites in the talc-free samples (Asemi-gawa: X_{Pi} = 0.18, X_{Ps} = 0.15, X_{Czo} = 0.67; Besshi: X_{Pi} = 0.09, X_{Ps} = 0.22, X_{Czo} = 0.69; cf. Tab. 3). The chemical composition of piemontite is mainly controlled by

Tab. 6 Representative analyses of piemontites at contact to garnet.

Point No.	95	96	97	3419	3319	3519	2191	1191	3191
Core/Rim	Core	Rim	Changed Rim	Core	Rim	Changed Rim	Core	Rim	Changed Rim
SiO_2 wt%	38.11 (0.04)	38.49	37.49	37.94	36.34	37.69	38.28	37.85	39.11
TiO_2	0.04 (0.00)	0.06	0.04	0.04	0.07	0.06	–	0.04	0.05
Al_2O_3	20.22 (0.03)	19.23	19.84	20.15	18.19	19.24	19.35	20.02	20.19
Fe_2O_3	5.40 (0.03)	8.50	5.49	5.88	9.38	9.08	9.32	5.98	7.02
Mn_2O_3	12.16 (0.03)	11.63	12.87	12.00	12.88	13.58	11.73	11.52	13.07
CaO	22.23 (0.03)	18.91	21.89	23.11	19.45	19.29	19.92	22.86	20.25
Total	98.16	96.82	97.62	99.12	96.31	98.94	98.60	98.27	99.69
No. of cations based on O = 25									
Si	3.05	3.10	3.00	3.02	3.00	3.02	3.05	3.02	3.08
Ti	0.002	0.004	0.002	0.002	0.004	0.003	–	0.002	0.003
Al	1.91	1.83	1.89	1.90	1.77	1.82	1.84	1.90	1.87
Fe^{3+}	0.32	0.51	0.33	0.35	0.58	0.54	0.56	0.36	0.41
Mn^{3+}	0.74	0.64	0.77	0.73	0.64	0.63	0.71	0.70	0.71
Total	2.972	2.984	2.99	2.982	2.994	2.99	3.11	2.962	2.993
Ca	1.91	1.64	1.90	1.98	1.73	1.65	1.70	1.97	1.71
Mn^{2+}	–	0.07	0.02	–	0.17	0.19	–	–	0.07
Total	1.91	1.71	1.92	1.98	1.90	1.84	1.70	1.97	1.78
End members									
Pi	24.66	21.33	25.66	24.33	21.41	21.00	23.66	23.33	23.66
Ps	10.66	17.00	11.00	11.66	19.40	18.00	18.66	12.00	13.66
Czo	64.68	61.67	63.34	64.01	59.19	61.00	57.68	64.67	62.68

Numbers in parentheses indicate precision of each element. Other columns have similar precision as column one. All of the Mn and Fe are considered as Mn_2O_3 and Fe_2O_3. Mn^{2+} and Mn^{3+} are computed based on structural formula.

oxygen fugacity, bulk composition, pressure and temperature (KESKINEN and LIOU, 1979). To investigate the fO_2 effect, mineralogical and geochemical evidences were used. Braunite and hematite are two fO_2 indicator minerals in the studied samples, and they were analyzed in detail. The results showed that braunite and hematite are homogenous and that there is no difference on chemical compositions of braunite and hematite between the Asemi-gawa and the Besshi areas. In fact, both areas are located within oxidized assemblage according to the CHOPIN (1978) definition because Mn^{3+} is present in the minerals such as piemontite and braunite, while Mn^{2+} is mostly incorporated in spessartine. Thus, the oxygen fugacity is inferred to be similar in the Asemi and Besshi areas. This conclusion was also supported by determining oxidation ratio ($Fe_2O_3 \times 100/(Fe_2O_3 + FeO)$) in the whole rock. In both areas, these ratios are around 100% (Tab. 7). Geochemical investigations on the Sanbagawa piemontite-quartz schists show that bulk compositions of the two areas are almost identical (Tab. 7). Therefore, the difference in composition of piemontite between the Asemi-gawa and Besshi areas must result from the difference in metamorphic grade. Thus, it appears that the epidote end-member component in piemontite increases from the garnet zone to the albite-biotite zone. Zoned crystals are good indicators of changing metamorphic conditions and are well-studied in the Sanbagawa belt (BANNO and SAKAI, 1989; OTSUKI and BANNO, 1990). Even though such observations in other minerals have been widely used to clarify metamorphic condition of the Sanbagawa belt, little attention has been given to chemical zonation of piemontite. This study shows that piemontite composition is sensitive to changing metamorphic grade. In the Sanbagawa belt, thus, the piemontite compositions show together with experimental results (KESKINEN and LIOU, 1979), that the chemical variation from core to rim in the talc-bearing and from core to mantle in the talc-free types may be related to prograde metamorphism. Additionally, the chemical trends from mantle to rim in the talc-free type may be attributed to the retrograde path of the Sanbagawa metamorphism.

Reaction relations between piemontite and spessartine

Based on textural and chemical criteria two different steps in the relation between piemontite and spessartine can be distinguished. The first step is the spessartine formation. Texturally, spessartine containing many inclusions of piemontite and braunite does not occur as a fine-grained matrix mineral but only as inclusion in albite porphyroblasts. On the other hand, textural relations indicate that braunite occurs as inclusion in spessartine or as a matrix mineral close to the core of piemontite from the talc-bearing type. Therefore, it may coexist with the piemontite core. The partitioning of Mn^{3+}, Fe^{3+} and Al between piemontite (Pi) and braunite (Br) confirms the assumption of

their coexistence. Distribution coefficients have been calculated by the equations:

$$[K_{D(Al\text{-}Mn)} = (X_{Al}/X_{Mn})_{Pi}/(X_{Al}/X_{Mn})_{Br}$$
$$X_{Al} = Al / Al + Mn]$$
$$[K_{D(Fe\text{-}Mn)} = (X_{Fe}/X_{Mn})_{Pi}/(X_{Fe}/X_{Mn})_{Br}$$
$$X_{Mn} = Mn / Fe + Mn]$$

showing that relative to braunite, piemontite is enriched in Al and Fe^{3+} and depleted in Mn^{3+} (Fig. 7). From the textural observations it is concluded that spessartine may be formed through a reaction involving piemontite and braunite. Experimental work by KESKINEN and LIOU (1979) shows that spessartine is a product of piemontite breakdown due to increasing temperature and/or decreasing oxygen fugacity. Thus, spessartine formation may be formed during the prograde path of the Sanbagawa metamorphism.

The second step is the changing chemical composition of piemontite at contact to spessartine.

Tab. 7 Representative bulk composition of piemontite-quartz schists in the Sanbagawa belt.

	Besshi area		Asemi area
Sample no.	1-1aQ	B4C	1213
SiO_2 wt%	75.67	78.05	78.26
TiO_2	0.37	0.45	0.4
Al_2O_3	5.77	8.01	7.33
Fe_2O_3	3.49	3.7	3.46
FeO	0.17	0.15	0.1
MnO	0.19	0.18	0.22
MgO	2.78	2.15	2.94
CaO	1.53	1.61	1.24
Na_2O	1.19	1.36	1.29
K_2O	0.61	1.03	0.72
P_2O_5	0.18	0.15	0.17
L.O.I.	6.95	2.6	2.97
Total	98.9	99.44	99.1
Oxidation Ratio*	95.36	96.1	97.19

*$Fe_2O_3 \times 100/(FeO + Fe_2O_3)$

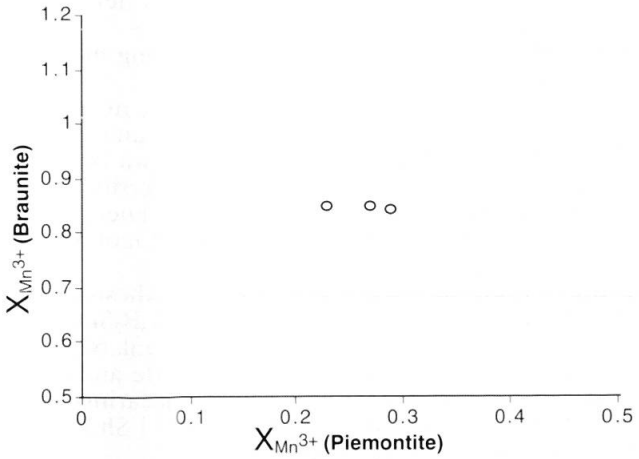


Fig. 7 Distribution of Mn^{3+} between coexisting piemontite and braunite.

Although, the preservation of compositional zoning of Al, Mn and Fe in zoned piemontite is a primary feature produced during growth, there may be some evidences of secondary cation exchange: in the talc-bearing types, for example, the chemical composition of piemontite changes whenever it occurs as inclusion in spessartine or in contact to it in matrix. This change was observed in the rim in a very limited area, about 33 μm away from the piemontite-spessartine contact. At the contact, piemontite tends to be, on average, richer in Mn ($X_{Pi} = 0.24$) and poorer in Fe and Ca ($X_{Czo} = 0.62$ and $X_{Ps} = 0.13$) as compared to rim ($X_{Pi} = 0.22$, $X_{Czo} = 0.62$, $X_{Ps} = 0.16$; cf. Tab. 6 and Fig. 8). Chemical change can also be seen at the piemontite-spessartine contact of the garnet, where it becomes richer in Ca and Fe ($X_{Grs} = 0.18$, $X_{And} = 0.09$) and poorer in Mn ($X_{Sps} = 0.73$) compared to the inner part ($X_{Sps} = 0.85$, $X_{Grs} = 0.10$, $X_{And} = 0.09$; cf. Tab. 4 and Fig. 8).

Although charge balance calculations in garnets are equivocal, the distribution of cations in the structure of studied garnet did not show any incorporation of trivalent Mn in the octahedral sites (Tab. 4). Indeed, for the mentioned fo_2 conditions, in which Mn can be present both as Mn^{2+} and Mn^{3+}, all of the available Mn^{3+} was preferably incorporated in the braunite or piemontite structure and there is no excess of Mn^{3+} to contribute

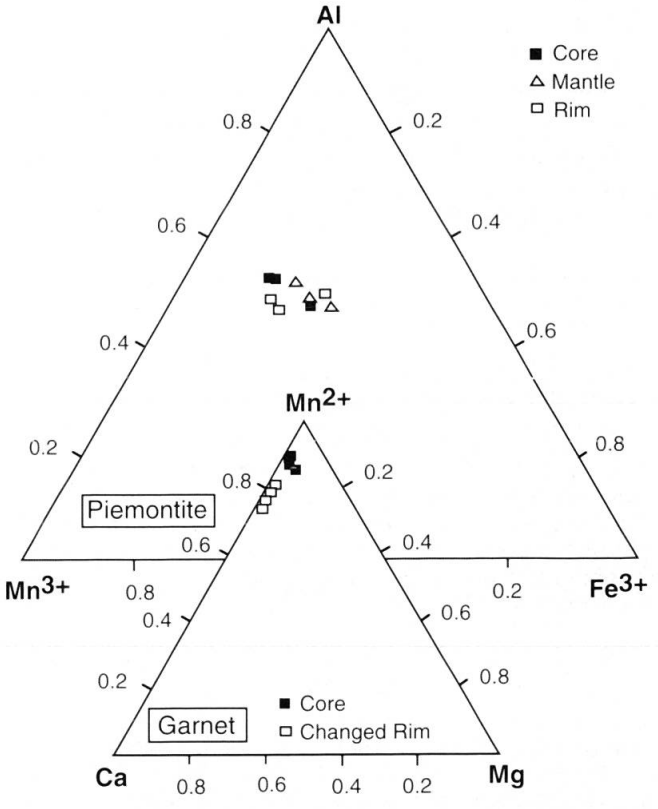


Fig. 8 Compositional variation of piemontite at the contact to spessartine.

to the garnet structure. Also, this conclusion is well supported by the fact that Mn^{3+}-bearing garnets have been synthesized only at pressure higher than 25 kbar (NISHIZAWA and KOIZOMI, 1975) which is very different from the Sanbagawa metamorphic condition. Furthermore, optical absorption spectra and theoretical considerations suggest that Mn is almost totally divalent in garnet structure (FRENTRUP and LANGER, 1982).

Concluding remarks

The following results were obtained from the petrographic and mineralogical study on piemontite-quartz schists from the Sanbagwa metamorphic belt:

(1) Piemontites of variable composition and complex chemical zoning are the most abundant Mn-silicates in highly oxidized Mn-rich quartz schists.

(2) The Asemi-gawa piemontites are richer in piemontite component than those from the Besshi area. The difference of metamorphic grade indicates that piemontite with higher epidote contents is stable at higher grade because bulk composition and oxygen fugacity are similar in both areas.

(3) Preservation of Mn, Al, Ca and Fe zoning in piemontite provides the best opportunity to unravel the metamorphic history of the region. The chemical evolution of piemontite can be compared with minerals like garnet. This study revealed prograde and retrograde paths of the Sanbagawa metamorphism.

(4) Besides piemontite, other Mn–Al–Ca silicates are also sensitive to changing metamorphic conditions. In the Sanbagawa belt, spessartine formation and cation exchange between spessartine and piemontite are examples of such sensitivity.

Acknowledgements

The results presented here are part of the author's doctoral thesis. The author wishes to express appreciation to Emeritus Prof. S. Banno and Doctors T. Hirajima and K. Tomita for their valuable helps and critical discussions during the time spent at Kyoto university. The author would like to express his sincere thanks to Prof. R. Gieré for his critical comments on several versions of this manuscript. This study was generously supported by the Ministry of Education of Japan.

References

ANASTASIOU, P. and LANGER, K. (1976): Synthese und Stabilität von Piemontit, $Ca_2Al_{3-p}Mn^{3+}_p(Si_2O_7/SiO_4/O/OH)$. Fortschr. Mineral., 54, Bh. 1, 3–4.

ANASTASIOU, P. and LANGER, K. (1977): Synthesis and physical properties of piemontite $Ca_2Al_{3-p}Mn^{3+}_p(Si_2O_7/SiO_4/O/OH)$. Contrib. Mineral. Petrol., 60, 225–245.

BANNO, S. and SAKAI, C. (1989): Geology and metamorphic evolution of the Sanbagawa metamorphic belt, Japan. In: DALY, J.S., CLIFF, R.A. and YARDLEY, B.W.D. (eds): Evolution of metamorphic belts. Geol. Soc. Spec. Pub., 43, 519–532.

CHOPIN, C. (1978): Les paragenèses réduites ou oxydées de concentrations manganésifères des "schistes lustrés" de Haute-Maurienne (Alpes françaises). Bull. Minéral., 101, 514–531.

DEER, W.A., HOWIE, R.A. and ZUSSMAN, J. (1992): An introduction to rock forming minerals. Longman Scientific & Technical, 2nd edition, 549 pp.

ENAMI, M. (1983): Petrology of pelitic schists in the oligoclase-biotite zone of the Sanbagawa metamorphic terrain, Japan: phase equilibria in the highest grade zone of a high-pressure intermediate type of metamorphic belt. J. Metamorphic Geol., 1, 141–161.

ENAMI, M., WALLIS, S.R. and BANNO, Y. (1994): Paragenesis of sodic pyroxene-bearing quartz schist: implication for the P-T history of the Sanbagawa belt. Contrib. Mineral. Petrol., 116, 182–198.

FRENTRUP, K.R. and LANGER, K. (1982): Microscope absorption spectrometry of silicate microcrystals in the range 4000–5000 cm^{-1} and its application to garnet end-members synthesized at high pressures. In: SCHREYER, W. (ed.): High pressure research in geoscience. Schweizerbart, Stuttgart, 247–258.

HIGASHINO, T. (1975): Biotite zone of Sanbagawa metamorphic terrain in the Siragayama area, central Shikoku, Japan. J. Geol. Soc. Japan, 81, 653–670.

HIGASHINO, T. (1990): The higher grade metamorphic zonation of the Sanbagawa metamorphic belt in central Shikoku, Japan. J. Metamorphic Geol., 8, 413–423.

HIRAJIMA, T. and BANNO, S. (1991): Electron-microprobe analysis of rock forming minerals with Kevex-delta IV (Quantum detector). Hitachi Scientific Instrument News, 34, 2–7.

HOLDWAY, M.J. (1972): Thermal stability of Al–Fe epidotes as a function of fO_2 and Fe content. Contrib. Mineral. Petrol., 37, 307–340.

IZADYAR, J., HIRAJIMA, T. and NAKAMURA, D. (2000): Talc-phengite-albite assemblage in piemontite-quartz schists of the Sanbagawa metamorphic belt, central Shikoku, Japan. Island Arc, 9, 145–158.

KAWACHI, Y., GRAPES, R.H., COOMBS, D.S. and DOWSE, M. (1983): Mineralogy and petrology of a piemontite-bearing schist, western Otago, New Zealand. J. Metamorphic Geol., 1, 353–372.

KESKINEN, M. and LIOU, J.G. (1979): Synthesis and stability relations of Mn–Al piemontite. Amer. Mineral., 64, 317–328.

KRETZ, R. (1983): Symbols for rock-forming minerals. Amer. Mineral., 63, 1023–1052.

MINAKAWA, T. (1992): Study on characteristic mineral assemblages and formation process of metamorphosed manganese ore deposit in the Sanbagawa belt. Memorial of Faculty of Science, Ehime University, 1, 1–74.

MORI, K. and KANEHIRA, K. (1984): X-ray energy spectrometry for electron probe analysis. J. Geol. Soc. Japan, 90, 271–285.

NISHIZAWA, H. and KOIZUMI, M. (1975): Synthesis and infrared spectra of $Ca_3Mn_2Si_3O_{12}$ and $Cd_3B_2Si_3O_{12}$ (B: Al, Ga, Cr, V, Fe, Mn) garnets. Amer. Mineral., 60, 84–87.

OTSUKI, M. and BANNO, S. (1990): Prograde and retrograde metamorphism of hematite-bearing basic schists in the Sanbagawa belt in central Shikoku. J. Metamorphic Geol., 8, 425–439.

REINECKE, T. (1986): Crystal chemistry and reaction relation of piemontites and thulites from highly oxidized

low grade metamorphic rocks at Vitali, Andros Islannd, Greece. Contrib. Mineral. Petrol., 93, 56–76.

SMITHH, D. and ALBEE A. (1967): Petrology of a piemontitee-bearing gneiss, San Gorgonio Pass, California. Ccontrib. Mineral. Petrol., 16, 189–203.

TAKAASU, A., WALLIS, S.R., BANNO, S. and DALLMEYER, R.D. (1994): Evolution of the Sanbagawa metamorphhic belt, Japan. Lithos, 33, 119–133.

WALLLIS, S.R. and BANNO, S. (1990): The Sanbagawa belt – treends in research. J. Metamorphic Geol., 8, 393–399.

WALLIS, S.R., BANNO, S. and RADVANCE, M. (1992): Kinematics, structure and relationship to metamorphism of east–west flow in the Sanbagawa belt southwest, Japan. Island Arc, 1, 176–185.

Manuscript received March 28, 1999; revision accepted February 28, 2000.